https://doi.org/10.3311/PPci.22319

Periodica Polytechnica Civil Engineering, 68(1), pp. 97–106, 2024

Deflection of a Partially Composite Beam Considering the Effect of Shear Deformation

Hamli Benzahar Hamid[1*], Chabaat Mohamed[2], Ayas Hillal[2]

[1] Acoustics and Civil Engineering Laboratory, Faculty of Sciences and Technology, Khemis Miliana University, Road of Theniet el Had, Khemis Miliana 44225, Algeria
[2] Built Environment Research Laboratory, Department of Structures and Materials, Civil Engineering Faculty, University of Sciences and Technology Houari Boumediene, B.P. 32 El-Alia, Bab Ezzouar, 16111 Algiers, Algeria
[*] Corresponding author, e-mail: hamli-zahar@univ-dbkm.dz

Received: 02 April 2023, Accepted: 24 July 2023, Published online: 25 August 2023

Abstract

In this research, the deflection in the interface of a partially composite beam considering the effect of shear deformation is determined. The system of beams is structured by two beams of prismatic sections, connected by an adhesive very thin and rigid, subjected to a uniform bending moment and a uniformly distributed load. The governing differential equation of the partially composite beam is obtained from the total functional energy that takes into consideration the shear deformation. The extreme moments creating second moments, shear forces and normal forces are applied to each beam. The differential equation is derived and then, compared to the one found in partial composite beams where the shear deformation is neglected. It is shown that the theoretical results of deflection with and without shear deformation are compared to each other and also with those found in the Timoshenko's beam theory.

Keywords

partially composite beam, shear deformation, deflection, differential equation

1 Introduction

Composite elements (beams, columns, diagonals) are mostly made of material with ductile or brittle behavior and are used, in civil engineering, for structures of reinforced concrete and metal frame [1–3]. The system of partially composite beam (PCB) is found in the case of the connection of beams with sail (reinforced concrete structures) and also in the case of mixed structures (steel-concrete). PCB proposed in this study is structured by two prismatic beams of different sections, superposed and assembled between them. In general, the connection between the beams is provided by bolts, rivets, welding or adhesive [4–6]. In the present research work, the assembly of the PCB is provided by a very thin adhesive which is stressed by shearing, bending, compression and traction with existing shear deformation. The normal force in each individual beam has a non-zero value, however, using the boundary conditions in which the normal force in the individual beam is generally assumed to disappear at the end of PCB [7]. The bending moment soliciting the PCB is a force torque. If one of the two beams is subjected to an axial force, then it produces an eccentric bending moment eccentric with respect to the gravity center of PCB [8, 9]. Nevertheless, to be comparable with the theory of PCB, these loads are presented in the form of axial load applied at the gravity center of PCB soliciting its whole cross section. The distribution of internal forces at the PCB boundaries is then evaluated as the difference between forces obtained at the extremities from the theoretical analysis of the distribution of forces at the extremities with those of the actual distribution of these efforts applied at the boundary [10, 11]. PCB behavior is based on the relationship between tangential forces and inelastic propagation of fracture [12–14].

This paper deals with the analysis of a partial composite beam under bending solicitation, based on the total functional energy of PCB (Eq. (12)). Taking into account in this equation the shear deformation (γ'), a governing differential equation of deflection is found and compared to the one obtained by Challamel and Girhammar [9] where the shear deformation is neglected. The shear deformation effect on the fully composite beam is also treated in this study, the main results are compared with those found in the Timoshenko's beam theory.

Cite this article as: Hamid, H. B., Mohamed, C., Hillal, A. "Deflection of a Partially Composite Beam Considering the Effect of Shear Deformation", Periodica Polytechnica Civil Engineering, 68(1), pp. 97–106, 2024. https://doi.org/10.3311/PPci.22319

2 Geometrical characteristics of the proposed PCB

In Fig. 1, all the geometrical characteristics of the sandwich beam are well described. The system is a superposition of two prismatic beams whose dimensions and forces are clearly shown. The first beam is denoted by the index 1 as B_1 and the second beam corresponds to the index 2 as B_2. Then, the whole system is considered partially composite. u, v, w are the displacements taken along the principal axes X, Y, Z, respectively. M_0 is the bending moment applied at the extremities of the system of PCB. M_1 and M_2 are seconds individually bending moments applied on the upper and lower beam, respectively. N_1, N_2 are the normal forces generated by the seconds bending moments applied on the upper and lower beam, successively. c.g.1 and c.g.2 correspond to the center of gravity of the upper and lower beam, respectively. c,g.PCB is the center of gravity of the partially composite beam.

On the other hand, h_1 and h_2 are the heights of upper and lower beam, respectively. b_1, b_2 correspond to the width of the upper and lower beam. d_1, d_2 are the distances between (c.g.1 and c.g.PBC), (c.g.1 and c.g.PBC), respectively.

The overall axial rigidity of PCB is given by $EA_0 = E_1A_1 + E_2A_2$, with E, E_1 and E_2 are the longitudinal elastic modulus of PCB, the upper and lower beam, respectively. Besides, A_0, A_1 and A_2 define the PCB section, the upper and lower beam, respectively. The center of the section of the lower beam is given by y c.g $= E_2A_2d_0/EA_0$ with $d_0 = d_1 + d_2$ corresponding to the distance between the two centers of gravity (c.g.1 and c.g.2).

All the parameters described previously are related by the following formula derived by Girhammar [15]:

$$\alpha_T^2 = K_T\left(\frac{1}{E_1A_1} + \frac{1}{E_2A_2} + \frac{d_0^2}{EI_{Z,0}}\right), \beta_T = K_T\frac{d_0}{EI_{Z,0}} \tag{1}$$

2.1 Interface and boundary conditions

It is obvious that composites whose fibers and matrices are brittles can show a fairly high resistance to fracture when the latter occurs along the interface before failure of the fibers [16–18]. Most of the important mechanisms of hardening are a result of the direct failure (shearing) of the interface [19]. This mechanism is at the origin of energy absorption with sustained stability of crack propagation [20, 21]. On the other hand, the tensile mode induces unstable fracture with limits of energy absorption [22, 23]. Therefore, the strength of the compound can be determined by optimizing the interface properties between the reinforcing fibers and the matrix phase [24, 25]. The two beams forming PCB are interconnected by a very thin adhesive with a high performance (good cohesion, mechanical strength and thermal). To obtain a durable assembly, the mechanical and physical characteristics must be comparable to those of parts to be assembled such as concrete, steel, wood, glass, etc. [26–28]. the glue used in this research work must be hard or dry, in order to give a strong bond and a high mechanical strength between the two materials. Fig. 2 shows three modes of bonding two beams by a thin adhesive [29, 30].

The beam above the interface ($Z > 0$) is denoted by the lower index 1, and the other one located in the lower part ($Z < 0$) by the index 2. For the present study, the conditions from the border to the interface are defined as follows [26]:

$$u_i^1\left(x, y, z = 0^+\right) = u_i^2\left(x, y, z = 0^-\right), \quad i = 1,2,3, \tag{2}$$

$$\sigma_{ij}^1\left(x, y, z = 0^+\right) = \sigma_{ij}^2\left(x, y, z = 0^-\right), \quad j = 1,2,3, \tag{3}$$

where, u_i (i = 1, 2, 3) is the displacement in the X, Y, Z directions, respectively. σ_{ij} (i, j = 1,2,3) is the component of the constraint in the X, Y, Z directions, respectively.

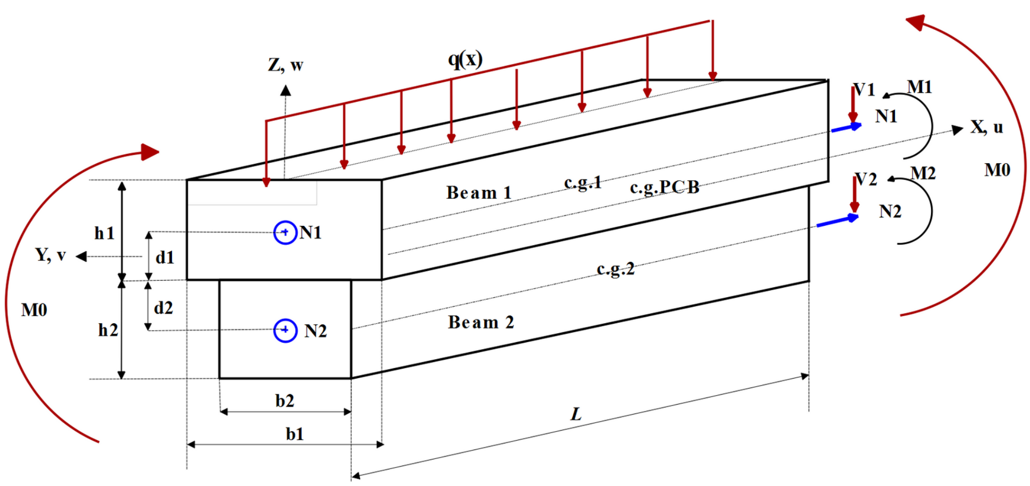

Fig. 1 PCB subjected to uniform bending moment and uniformly distributed load

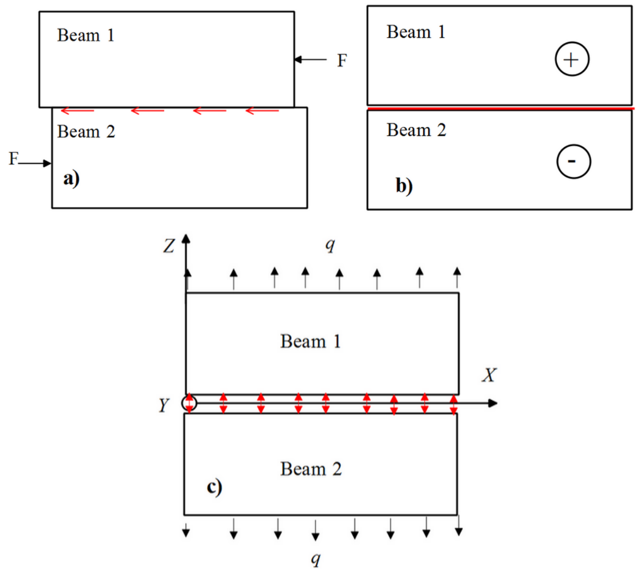

Fig. 2 Three modes of gluing: a) sliding in the plane, b) sliding out of plane, c) tensile

By applying the theory of a bi-material (composite actions) and neglecting the effects of the vertical separation between the two assembled materials, there are several experimental verifications that can be made [31–34]. For the complete composite action, the shearing modulus tends to infinity ($K_T \to \infty$), on the other hand, in the case of a non-composite action, the shearing modulus tends to zero ($K_T \to 0$). For the PCB system, the bonding layer between two beams is stressed by a shearing force given by the following relation:

$$K_T = \frac{bG}{e}, \tag{4}$$

where G is the shear modulus. e, b are the thickness and the width of the bonding layer (adhesive), respectively.

3 Stress in partially composite beams

According to Fig. 1, the PCB system is loaded by the moments (M_0 the global moment at the ends on either side, M_1 and M_2, seconds individually moments at the upper and lower beams, respectively) and on the other side by the shear forces V_1 and V_2 that affect the sections of the upper and lower beam, respectively. It is obvious that N_1 and N_2 corresponding to the normal forces are created by the global moment M_0 applied individually to the sections of the upper and lower beam, respectively. Thus, shear deformation is considered for composite and partially composite beams [35, 36]. Assuming that the deflection curves of the two beams are equal, the differential equation should confirm the relationship provided by Girhammar and Gopu [37]:

$$N_2 = \left(1 - \frac{EI_{Z,0}}{EI_{Z,\infty}}\right) . \frac{M_0}{d_0}; \; N_1 = -\left(1 - \frac{EI_{Z,0}}{EI_{Z,\infty}}\right) . \frac{M_0}{d_0} . \tag{5}$$

The following boundary conditions are satisfied:

$$N_1(0) = N_1(L) = 0 . \tag{6}$$

4 Boundary layer effect

The loaded systems must be equilibrated at their ends. According to the PCB shown previously in Fig. 1, the equilibrium equations of the forces are as follows:

$$M_0 = M_1 + M_2 - N_1 d_0 , \tag{7}$$

$$N_1 + N_2 = 0 . \tag{8}$$

Since the assumptions of linear and nonlinear elasticity stand for this research study, then normal forces and bending moments can be written in the following form:

$$N_1 = E_1 A_1 u_1' , \tag{9}$$

$$N_2 = E_2 A_2 u_2' , \tag{10}$$

$$y = \iint \frac{M_1(x)}{E_1 I_1} dx^2 = \iint \frac{M_2(x)}{E_2 I_2} dx^2 , \tag{11}$$

where, y is the deflection of beams.

5 Differential equation of PCB

Differential equations of the PCB with a shear deformation subjected to a uniform bending moment and uniformly distributed load are obtained from the total energy as follows:

$$U(u_1, u_2, v) = \int_0^L \begin{bmatrix} \frac{1}{2} EI_{Z,0} (v'')^2 + \frac{1}{2} E_1 A_1 (u_1')^2 \\ + \frac{1}{2} E_2 A_2 (u_2')^2 + \frac{1}{2} beG\gamma^2 \\ + \frac{1}{2} a (be)^2 G\gamma'^2 \end{bmatrix} dx \tag{12}$$

$$+ M_0 \left[v'(L) - v'(0) \right] - \int_0^L qv\, dx,$$

where, G corresponds to the shear modulus of the adhesive, γ' is the shear deformation and a is a constant value. For a complete composite action, the shearing modulus tends to infinity ($a \to \infty$), on the other hand, for a non-composite action the shearing modulus tends to zero ($a \to 0$). This last equation assumes that the curvature of the two sub-elements (upper and lower beam) is equal. Let's derive Eq. (12) and substitute both Eq. (9) and Eq. (10), one can get an equation of a stationary energy leading to the principle of virtual work as follows:

$$\delta(U)=\int_0^L\left[EI_{Z,0}(v'')\delta(v'')+N_1\delta u_1'+N_2\delta u_2'+be\tau\delta\gamma+a(be)^2\tau'\delta\gamma'\right]$$
$$dx+M_0\left[\delta v'(L)-\delta v'(0)\right]-\int_0^L q\delta v dx=0 \tag{13}$$

where

$$\tau=\gamma G,\gamma=\left(\frac{u_2-u_1}{e}\right)+\frac{d_0}{e}v'. \tag{14}$$

Integration by parts of Eq. (13) leads us to the following system of differential equations (see Appendix C).

$$EI_{Z,0}\left(v^{(4)}\right)-b\tau'd_0+ab^2\tau'''d_0-q=0 \tag{15}$$

$$\left[\left(EI_{Z,0}(v'')+ab^2e\tau'd_0+M_0\right)\delta v'\right]_0^L=0 \tag{16}$$

$$N_1'-b\tau+ab^2e\tau''=0 \tag{17}$$

$$N_2'-ab^2e\tau''+b\tau=0 \tag{18}$$

Substitution of both Eqs. (17) and (18) into Eq. (15) and using the second derivative, we find the following differential equation (see Appendix B).

$$x^4-\frac{\alpha_T^2}{\left(1+abe\alpha_T^2\right)}x''+\left(\frac{\alpha_T^2}{EI_{Z,\infty}\left(1+abe\alpha_T^2\right)}\right)M''$$
$$-\left(\frac{a^2be\alpha_T^2}{EI_{Z,\infty}}+\right)\frac{M^4}{\left(1+abe\alpha_T^2\right)}=0 \tag{19}$$

Using the integration, Eq. (19) can be written as follows:

$$\left[x-\left(\frac{\left(1+abe\alpha_T^2\right)}{\alpha_T^2}\right)x''\right]$$
$$=\left(\frac{1}{EI_{Z,\infty}}\right)M-\left(\frac{abe\alpha_T^2EI_{Z,0}+EI_{Z,\infty}}{\alpha_T^2EI_{Z,\infty}EI_{Z,0}}\right)M''. \tag{20}$$

It is obvious that in the case where $a = 0$, Eq. (20) takes the form as the one found in [9]:

$$\left(\frac{\alpha_T^2}{EI_{Z,\infty}}\right)M-\left(\frac{M''}{EI_{Z,0}}\right)=\alpha_T^2x-x''. \tag{21}$$

In this research study, the moments are uniform then $M(x) = M_0$ which leads to $M'' = 0$. Using these assumptions, previous Eq. (20) becomes:

$$x-\left(\frac{\left(1+abe\alpha_T^2\right)}{\alpha_T^2}\right)x''=\left(\frac{M}{EI_{Z,\infty}}\right). \tag{22}$$

The corresponding solution to previous Eq. (22) is given as follows:

$$v''(x)=\frac{M}{EI_{Z,\infty}}e^{-\sqrt{\frac{\mu_T^2}{1+abe\mu_T^2}}x}. \tag{23}$$

Substitution of Eq. (5), Eq. (9), Eq. (10) in Eq. (16), lead us to a simplified expression of the curvature:

$$v''(x)=-\frac{M_0+ab^2.G\left(1-\frac{EI_{Z,0}}{EI_{Z,\infty}}\right).M_0\cdot\frac{EA_0}{EA_p}}{EI_{Z,0}+a.b^2.G.d_0^2}. \tag{24}$$

On the other side, if we substitute Eq. (23) into Eq. (24), then, the bending moment takes the form:

$$M=EI_{Z,\infty}\left\{\frac{\left(M_0+ab^2.G\left(1-\frac{EI_{Z,0}}{EI_{Z,\infty}}\right).M_0\cdot\frac{EA_0}{EA_p}\right)}{\left[EI_{Z,0}+ab^2.G.d_0^2\right]}-1\right\}. \tag{25}$$

Let's substitute Eq. (25) into Eq. (23) and integrate, the deflection becomes:

$$v(x)=\left\{\frac{\left(M_0+ab^2.G\left(1-\frac{EI_{Z,0}}{EI_{Z,\infty}}\right).M_0\cdot\frac{EA_0}{EA_p}\right)}{\left[EI_{Z,0}+ab^2.G.d_0^2\right]}\right\}\frac{\left(L.x-x^2\right)}{2}. \tag{26}$$

In the absence of the shear deformation (a = 0), the deflection can be written under the following form:

$$v(x)_{a\to0}=\left\{\frac{M_0}{EI_{Z,0}}\right\}\frac{\left(L.x-x^2\right)}{2}. \tag{27}$$

On the other hand, the presence of the shear deformation ($a \to \infty$) can stiffen the PCB system by inertia $EI_{Z,\infty}$ as (see Appendix B for more details).

$$v(x)_{a\to\infty}=\left\{\left(\frac{M_0}{EI_{Z,\infty}}\right)\right\}\frac{\left(L.x-x^2\right)}{2} \tag{28}$$

Taking into account the shear deformation, previous Eq. (26) is determined as a function of the shear modulus (G) and the width of the bonding layer as well as the geometrical characteristics of the section of PCB system such as $EI_{Z,0}$, $EI_{Z,\infty}$, EA_0, EA_p and d_0. In the absence of shear deformation, Eq. (27) is written as a function of the inertia $EI_{Z,0}$, meaning a superposition of two unrelated beams. On the other hand, one can notice that for the case of a shear deformation at infinity, Eq. (28) is derived as a function of the PCB section inertia ($EI_{Z,\infty}$) which is considered as a superposition of the two beams linked together.

Table 1 Deflection in case of both an existing and absence of shear deformation

PBC Length (x)	Deflection with shear deformation ($a \to \infty$)	Deflection without shear deformation ($a \to 0$)
0	0	0
$L/8$	$7.M_0.L^2/128.EI_{Z,\infty}$	$7.M_0.L^2/128.EI_{Z,0}$
$L/4$	$12.M_0.L^2/128.EI_{Z,\infty}$	$12.M_0.L^2/128.EI_{Z,0}$
$3L/8$	$15.M_0.v^2/128.EI_{Z,\infty}$	$15.M_0.L^2/128.EI_{Z,0}$
$L/2$	$16.M_0.L^2/128.EI_{Z,\infty}$	$16.M_0.L^2/128.EI_{Z,0}$
$5L/8$	$15.M_0.L^2/128.EI_{Z,\infty}$	$15.M_0.L^2/128.EI_{Z,0}$
$3L/4$	$12.M_0.L^2/128.EI_{Z,\infty}$	$12.M_0.L^2/128.EI_{Z,0}$
$7L/8$	$7.M_0.L^2/128.EI_{Z,\infty}$	$7.M_0.L^2/128.EI_{Z,0}$
L	0	0

The deflection can be determined in case of both an existing and absence of shear deformation. The following Table 1 summarized the deflections found in different sections of PCB.

Eq. (28) and Eq. (27) have proven that the presence of shear deformation increases the total inertia of PCB and consequently; decreases the deflection. In Eq. (26), the variation of the deflection can be determined according to the constant a. Fig. 3 represents the variation of the deflection $v(x)$ as a function of the length (L) of the PCB (case: $a = 0, 1, 2, 3, 4 + \infty$).

In the case of shear deformation, shear modulus (G) of the cohesive greatly influences the deflection of PCB. Fig. 4 shows the variation of the deflection as a function of the rate (G/E), at presence and absence of shear deformation.

6 Variation of the width of the lower beam

As shown in Fig. 1, keeping the section of the upper beam B_1 (h_1, b_1) and varying the width (b_2) of the lower beam, the deflection can be determined with the consideration of the presence of the shear deformation (a $\to \infty$) and at absence of this shear deformation ($a = 0$). For each width (b_2), the deflection without a shear deformation always remains greater than that taken with a shear deformation. Fig. 5 represents the variation of the deflection versus the rate (b_2/b_1) of widths of the two beams.

Fig. 4 shows the variation of the maximum deflection with the rate (G/E). One can notice from this curve that when a = 1 to 4, the deflection decreases while the rate (G/E) increases. For the case of an interface without a shear deformation ($a = 0$), the deflection is steady and can reach a maximum value meanwhile in the presence of a shear deformation ($a \to \infty$), the deflection is constant towards a minimum value as displayed in Fig. 5. Both curves show that the deflection decreases while the width's rate increases. It is obvious that the deflection rate (v_2/v_1) is proportional to the width's rate (b_2/b_1).

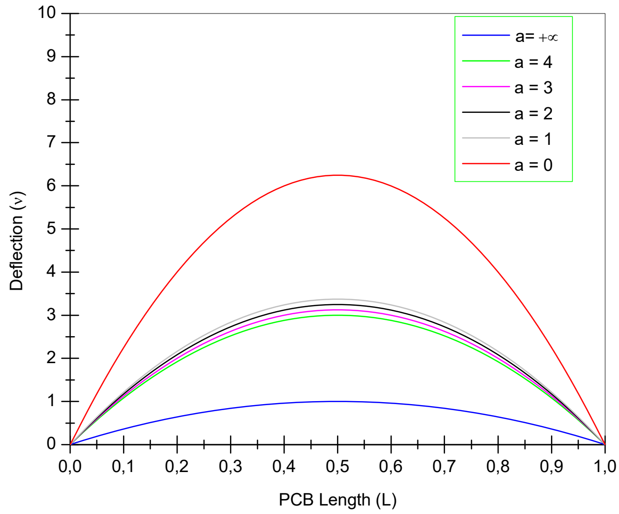

Fig. 3 Deflection $v(x)$ vs. the length of the PCB (Case: $a = 0, 1, 2, + \infty$)

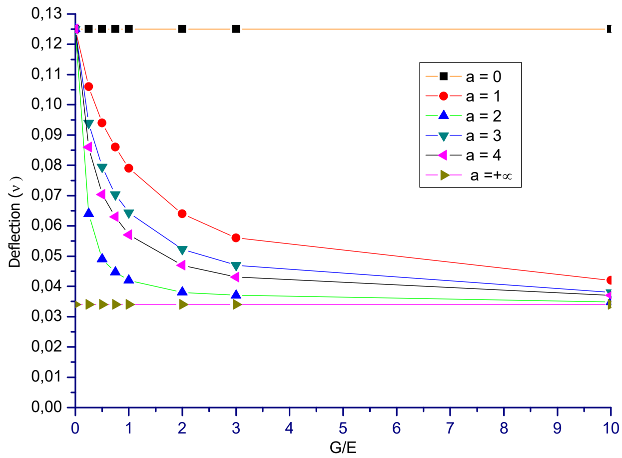

Fig. 4 Variation of the maximum deflection $v(L/2)$ vs. rate G/E (Case: $a = 0, 1, 2, 3, 4, + \infty$)

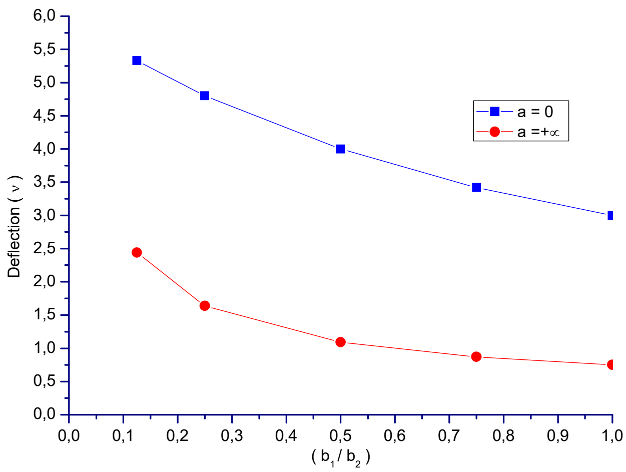

Fig. 5 PCB deflection at presence ($a \to \infty$) and absence ($a = 0$) of shear deformation

7 Rate of two deflections

For each cross section of PCB, deflection can be determined at an existing or not of the of shear deformation. The deflection with a shear deformation is noticed by n_1 and that without a shear deformation by n_2. The rate of both deflections (n_2/n_1) is determined on the basis of the variation of the width at the lower beam in comparison to that of the upper beam (b_2/b_1). Fig. 6 represents the variation of n_2/n_1 as a function of b_2/b_1.

8 Fully composite beam

It is assumed that a composite beam (CB) is structured by two identical beams having the same cross section (h, b) and a length L, subjected to a uniform bending moment and a uniformly distributed load (see, Fig. 7).

In case of a deflection without a shear deformation ($a = 0$), we get:

$$EI_{Z,0} = EI_1 + EI_2 = 2E\frac{b.h^3}{12} \text{ and } I_1 = I_2 = \frac{b.h^3}{12}. \tag{29}$$

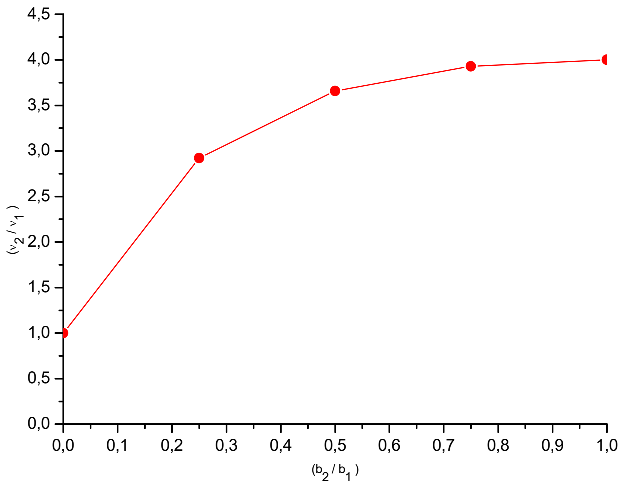

Fig. 6 Deflections rate (v_2/v_1) vs. (b_2/b_1)

And if we substitute Eq. (29) into Eq. (27), the deflection becomes as

$$v(x) = 3.\left[\frac{M_0}{E.b.h^3}\right]\left(L.x - x^2\right). \tag{30}$$

On the other hand, if we substitute Eq. (29) into Eq. (28), the presence of the shear deformation leads us to a deflection of two identical beams under the following form:

$$v(x) = \frac{3}{4}\left[\frac{M_0}{E.b.h^3}\right]\left(L.x - x^2\right). \tag{31}$$

In the case of a superposition of two identical prismatic beams and according to Eqs. (30) and (31), it is obvious that the presence of a shear deformation can decrease the deflection by four times which is compared with Timoshenko beam's theory. The Fig. 8 represents the deflection of the composite beam with and without shear deformation.

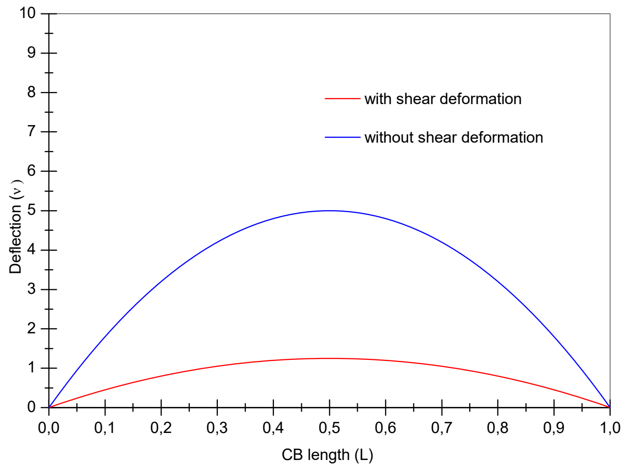

Fig. 8 Deflection $v(x)/[M_0{-}L^2/E.b^4]$ vs. the length of the composite beam with/without the shear deformation

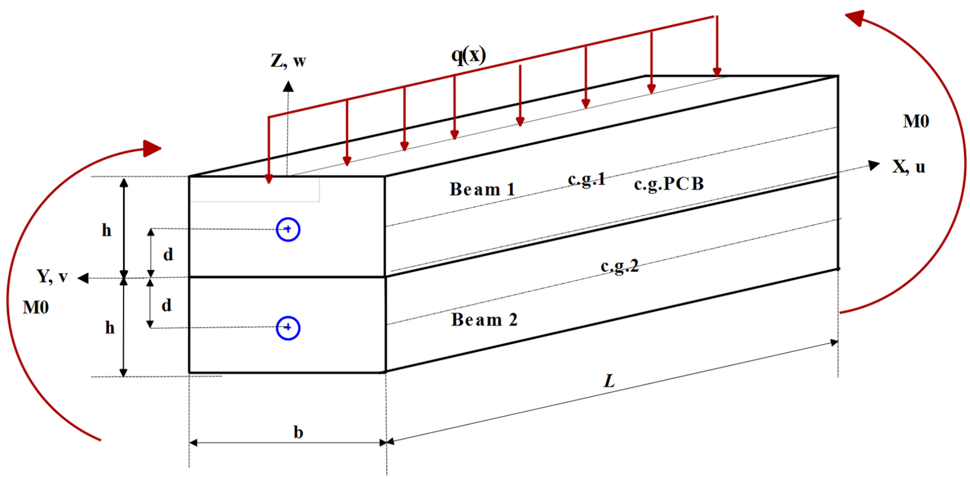

Fig. 7 Composite beam structured by two identical beams

9 Conclusion

Deflection in the PCB considering the shear deformation has been theoretically studied. In this study, PCB is subjected to uniformly distributed load and bending moments M_0 with existing shear deformation at the interface. Using the total functional energy, the governing differential equation of PCB is derived as a function of the shear deformation. Neglecting the term of the shear deformation in the global expression of deflection developed in this research, the resulting equation takes the form of a differential equation of the deflection of a PCB which is similar to the one formulated by Challamel and Girhammar [9]. It is shown that the general solution of the governing differential equation represents the second derivative of the deflection of PCB. Based on the boundary conditions and using the double integral, equation of the deflection with the shear deformation is obtained. One can notice that the variation of the deflection versus the shear deformation can decrease the deflection in the PCB. For a fully composite beam, it is noticed here that the presence of a shear deformation reduces the inertia and the deflection of CB by four times. This phenomenon is proven in the Timoshenko's beam theory.

Nomenclature

PCB	Partially Composite Beam
B_1, B_2	Upper and lower beam successively
n_1, n_2	Deflections of upper and lower beam successively
γ'	Shear deformation
M_0	Bending moment applied at the extremities of the system of PCB
M_1, M_2	Normal forces generated by the seconds bending moments applied on the upper and lower beam successively
N_1, N_2	Normal forces generated by the seconds bending moments applied on the upper and lower beam successively
A	Dimensionless parameter
e, b, q	Thickness and width of the bonding layer (adhesive) Uniformly distributed load
E_1, E_2	longitudinal elastic modulus of upper and lower beam successively
A_1, A_2	Section of upper and lower beam successively
I_1, I_2	Inertia's of upper and lower beam successively

References

[1] Wang, Y. C. "Deflection of Steel-Concrete Composite Beams with Partial Shear Interaction", Journal of Structural Engineering, 124(10), pp. 1159–1165, 1998. https://doi.org/10.1061/(ASCE)0733-9445(1998)124:10(1159)

[2] Hamli Benzahar, H. "Theoretical and numerical analysis of stress and stress intensity factor in bi-material", International Journal of Structural Integrity, 10(1), pp. 76–84, 2019. https://doi.org/10.1108/IJSI-08-2018-0048

[3] Schnabl, S., Planinc, I. "The effect of transverse shear deformation on the buckling of two-layer composite columns with interlayer slip", International Journal of Non-Linear Mechanics, 46(3), pp. 543–553, 2011. https://doi.org/10.1016/j.ijnonlinmec.2011.01.001

[4] Rizzoni, R., Dumont, S., Lebon, F., Sacco, E. "Higher order adhesive effects in composite beams", European Journal of Mechanics - A/Solids, 85, 104108, 2021. https://doi.org/10.1016/j.euromechsol.2020.104108

[5] Soto, A., Tehrani, F. M. "An Investigation of Crack Propagation in Steel Fiber-Reinforced Composite Beams", Periodica Polytechnica Civil Engineering, 62(4), pp. 956–962, 2018. https://doi.org/10.3311/PPci.10910

[6] Kim, S.-B., Cho, S.-H., Choi, Y.-H., Kim, S.-S. "An Experimental Study on Bending Performance of Hybrid Forming Composite Beam", International Journal of Steel Structures, 17(4), pp. 1641–1651, 2017. https://doi.org/10.1007/s13296-017-1228-3

[7] Tang, J., Chen, X., Yang, K. "Evaluating Structural Failure of Load-Carrying Composite Box Beams with Different Geometries and Load Conditions", Applied Composite Materials, 26(4), pp. 1151–1161, 2019. https://doi.org/10.1007/s10443-019-09776-4

[8] Tsai, M.-H. "Chord rotation demand for effective catenary action of RC beams under gravitational loadings", Structural Engineering and Mechanics, 58(2), pp. 327–345, 2016. https://doi.org/10.12989/sem.2016.58.2.327

[9] Challamel, N., Girhammar, U. A. "Boundary- layer effect in composite beams with interlayer slip", Journal of Aerospace Engineering, 24(2), pp. 199–209, 2011. https://doi.org/10.1061/(ASCE)AS.1943-5525.0000027

[10] Murakami, H. "A Laminated Beam Theory with Interlayer Slip", Journal of Applied Mechanics, 51(3), pp. 551–559, 1984. https://doi.org/10.1115/1.3167673

[11] Zhong, J., Yan, Q., Wu, J., Zhang, Z. "Mechanism research of slip effect between frictional laminated beams", Advances in Mechanical Engineering, 11(3), pp. 1–12, 2019. https://doi.org/10.1177/1687814019828461

[12] Blondeau, C., Pappas, G., Botsis, J. "Influence of ply-angle on fracture in antisymmetric interfaces of CFRP laminates", Composite Structures, 216, pp. 464–476, 2019. https://doi.org/10.1016/j.compstruct.2019.03.004

[13] Hammoudi, I., Touati, M., Chabaat, M. "Damage Propagation at the Interface of a Sandwich Beam", Periodica Polytechnica Civil Engineering, 66(3), pp. 681–693, 2022. https://doi.org/10.3311/PPci.19642

[14] Vo, T. P., Thai, T.-T. "Static behavior of composite beams using various refined shear deformation theories", Composite Structures, 94(8), pp. 2513–2522, 2012.
https://doi.org/10.1016/j.compstruct.2012.02.010

[15] Girhammar, U. A. "Composite beam-columns with interlayer slip-Approximate analysis", International Journal of Mechanical Sciences, 50(12), pp. 1636–1649, 2008.
https://doi.org/10.1016/j.ijmecsci.2008.09.003

[16] Adekola, A. O. "Partial interaction between elastically connected elements of a composite beam", International Journal of Solids Structure, 4(11), pp. 1125–1135 1968.
https://doi.org/10.1016/0020-7683(68)90027-9

[17] Haeri, H., Sarfarazi, V., Zhu, Z. "Effect of normal load on the crack propagation from pre-existing joints using particle flow code", Computers and Concrete, 19(1), pp. 99–110, 2017.
https://doi.org/10.12989/cac.2017.19.1.099

[18] Mantič, V., Távara, L., Blázquez, A., Graciani, E., París, F. "A linear elastic-brittle interface model: application for the onset and propagation of a fibre-matrix interface crack under biaxial transverse loads", International Journal of Fracture, 195(1), pp. 15–38, 2015.
https://doi.org/10.1007/s10704-015-0043-0

[19] Askarinejad, S., Thouless, M. D., Fleck, N. A. "Failure of a pre-cracked epoxy sandwich layer in shear", European Journal of Mechanics - A/Solids, 85, 104134, 2021.
https://doi.org/10.1016/j.euromechsol.2020.104134

[20] White, B. C., Story, W. A., Brewer, L. N., Jordon, J. B. "Fracture mechanics methods for evaluating the adhesion of cold spray deposits", Engineering Fracture Mechanics, 205(1), pp. 57–69, 2019.
https://doi.org/10.1016/j.engfracmech.2018.11.009

[21] Legendre, J., Créac'hcadec, R., Gilbert, F., Jacquet, D. "A new method to measure the adhesion capability of the metallic surface under shear loading using a modified Arcan test", The Journal of Adhesion, 94(12), pp. 1017–1035, 2018.
https://doi.org/10.1080/00218464.2017.1334557

[22] Yu, J., Wang, Y., Li, Z., Zhang, Q., Jian, X., Zhang, Z. "Using DIC technique to characterize the mode II interface fracture of layered system composed of multiple materials", Composite Structures, 230, 111413, 2019.
https://doi.org/10.1016/j.compstruct.2019.111413

[23] Chen, P., Wang, K.-Y., Huang, H.-H. "Strength and failure modes of adhesively bonded composite joints with easily fabricated non-flat interfaces", Composite Structures, 225, 111162, 2019.
https://doi.org/10.1016/j.compstruct.2019.111162

[24] Challamel, N., Andrade, A., Camotim, D., Milisavlevich, B. M. "On the flexural- torsional buckling of cantilever strip beam-columns with linearly varying depth", Journal of Engineering Mechanics, 136(6), pp. 787–800, 2010.
https://doi.org/10.1061/(ASCE)EM.1943-7889.0000121

[25] Davoodnabi, S. M., Mirhosseini, S. M., Shariati, M. "Behavior of steel-concrete composite beam using angle shear connectors at fire condition", Steel and Composite Structures, 30(2), pp. 141–147, 2019.
https://doi.org/10.12989/scs.2019.30.2.141

[26] Zhang, T.-Y., Li, J. C. M. "Interaction of an edge dislocation with an interfacial crack", Journal of Applied Physics, 72(6), pp. 2215–2226, 1992.
https://doi.org/10.1063/1.351614

[27] Kumar, R. R., Pandey, K. M., Dey, S. "Probabilistic assessment on buckling behavior of sandwich panel: - A radial basis function approach", Structural Engineering and Mechanics, 71(2), pp. 197–210, 2019.
https://doi.org/10.12989/sem.2019.71.2.197

[28] Luo, P., Zhang, Q., Bao, Y. "Predicting weld root notch stress intensity factors for rib-to-deck welded joint under deck loading modes", International Journal of Fatigue, 128, 105212, 2019.
https://doi.org/10.1016/j.ijfatigue.2019.105212

[29] Zhang, T., Meng, J., Pan, Q., Sun, B. "The influence of adhesive porosity on composite joints", Composites Communications, 15(1), pp. 87–91, 2019.
https://doi.org/10.1016/j.coco.2019.06.011

[30] Wang, Z.-Y., Shi, Y., Wu, Y., Wang, Q., Luo, S. "Shear behaviour of structural silicone adhesively bonded steel-glass orthogonal lap joints", Journal of Adhesive Science and Technology, 32(24), pp. 2693–2708, 2018.
https://doi.org/10.1080/01694243.2018.1501862

[31] Kroflič, A., Planinc, I., Saje, M., Turk, G., Čas, B. "Nonlinear analysis of two-layer timber beams considering interlayer slip and uplift", Engineering of Structures, 32(6), pp. 1617–1630, 2010.
https://doi.org/10.1016/j.engstruct.2010.02.009

[32] Ang, W.-T., Fan, H. "A hypersingular boundary integral method for quasi-static antiplane deformations of an elastic bimaterial with an imperfect and viscoelastic interface", Engineering Computations, 21(5), pp. 529–539, 2004.
https://doi.org/10.1108/02644400410543940

[33] Chowdhuri, M. A. K., Xia, Z. "Theory and experimental method to determine bonding strength envelope of bi-material interface", International Journal of Structural Integrity, 3(4), pp. 409–423, 2012.
https://doi.org/10.1108/17579861211281209

[34] Atashipour, S. R., Girhammar, U. A., Challamel, N. "Stability analysis of three-layer shear deformable partial composite columns", International Journal of Solids and Structures, 106, pp. 213–228, 2017.
https://doi.org/10.1016/j.ijsolstr.2016.11.018

[35] Girhammar, U. A., Pan, D. H. "Exact static analysis of partially composite beams and beam-columns", International Journal of Mechanical Sciences, 49(2), pp. 239–255, 2007.
https://doi.org/10.1016/j.ijmecsci.2006.07.005

[36] Wang, J., Qiao, P. "Fracture analysis of shear deformable bi-material interface", Journal of Engineering Mechanics, 132(3), pp. 306–316, 2006.
https://doi.org/10.1061/(ASCE)0733-9399(2006)132:3(306)

[37] Girhammar, U. A., Gopu, V. K. A. "Composite beam-columns with interlayer slip-exact analysis", Journal of Structures Engineering, 119(4), pp. 1265–1282, 1993.
https://doi.org/10.1061/(ASCE)0733-9445(1993)119:4(1265)

Appendix A

The axial flexural rigidity of PCB is given by:

$$EA_0 = E_1A_1 + E_2A_2 \,, \tag{A1}$$

$$EA_p = E_1A_1 \cdot E_2A_2 \,, \tag{A2}$$

$$I_0 = E_1I_1 + E_2I_2 \,, \tag{A3}$$

$$EI_\infty = EI_0 + \frac{EA_p d_0^2}{EA_0} \,. \tag{A4}$$

Appendix B

Eq. (13) becomes

$$\delta(U) = \int_0^L \begin{bmatrix} EI_{Z,0}(v'')\delta(v'') + N_1\delta u_1' + N_2\delta u_2' + b\tau d_0\delta v' + b\tau\delta u_2 \\ -b\tau\delta u_1 + ab^2e\tau'\delta u_2' - ab^2e\tau'\delta u_1' + ab^2e\tau' d_0\delta v'' \end{bmatrix} dx + M_0[\delta v'(L) - \delta v'(0)] - \int_0^L q\delta v dx = 0 \tag{B1}$$

where:

$$\begin{cases} \gamma = \left(\dfrac{u_2 - u_1}{e}\right) + \dfrac{d_0}{e}v' \\ \gamma' = \left(\dfrac{u_2' - u_1'}{e}\right) + \dfrac{d_0}{e}v'' \end{cases} \tag{B2}$$

$$\begin{cases} d\gamma = \left(\dfrac{\delta u_2 - \delta u_1}{e}\right) + \dfrac{d_0}{e}\delta v' \\ d\gamma' = \left(\dfrac{\delta u_2' - \delta u_1'}{e}\right) + \dfrac{d_0}{e}\delta v'' \end{cases} \tag{B3}$$

Eq. (19) becomes (with;)

$$(v^6) - \frac{\alpha_T^2}{\left(1 + abe\alpha_T^2\right)}\left(v^4\right) + q\left(\frac{\alpha_T^2}{EI_{Z,\infty}\left(1 + abe\alpha_T^2\right)}\right) - \frac{q''}{\left(1 + abe\alpha_T^2\right)}\left(\frac{abe\alpha_T^2}{EI_{Z,\infty}} + \frac{1}{EI_{Z,0}}\right) = 0 \tag{B4}$$

Eq. (28) becomes:

$$\lim_{a\to\infty} v(x) = \left\{ \frac{a\left(\dfrac{M_0}{a} + b^2.G\left(1 - \dfrac{EI_{Z,0}}{EI_{Z,\infty}}\right).M_0 \cdot \dfrac{EA_0}{EA_p}\right)}{a\left[\dfrac{EI_{Z,0}}{a} + b^2.G.d_0^2\right]} \right\} \frac{\left(L.x - x^2\right)}{2} \tag{B5}$$

where:

$$\left(EI_{Z,\infty} - EI_{Z,0} = EA_p h_0^2 / EA_0\right) \tag{B6}$$

Appendix C
Integration of differential equation

In Eq. (13), the integrations by parts can be rewritten in the following form:

$$\left[\left(-EI_{Z,0}\left(v'''\right)+b\tau d_0-ab^2e\tau''d_0\right)\delta\left(v\right)\right]_0^L=0\,, \tag{C1}$$

$$\left[\left(N_1-ab^2e\tau'\right)\delta u_1\right]_0^L=0\,, \tag{C2}$$

$$\left[\left(N_2-ab^2e\tau'\right)\delta u_2\right]_0^L=0\,. \tag{C3}$$

From where:

$$\int_0^L EI_{Z,0}\left(v''\right)\delta\left(v''\right)=\left[EI_{Z,0}\left(v''\right)\delta\left(v'\right)-EI_{Z,0}\left(v'''\right)\delta\left(v\right)\right]_0^L+\int_0^L EI_{Z,0}\left(v^{(4)}\right)\delta\left(v\right)dx=0\,, \tag{C4}$$

$$\int_0^L N_1\delta u_1'=\left[N_1\delta u_1\right]_0^L\int_0^L N_1'\delta u_1'dx=0\,, \tag{C5}$$

$$\int_0^L N_2\delta u_2'=\left[N_2\delta u_2\right]_0^L\int_0^L N_2'\delta u_2'dx=0\,, \tag{C6}$$

$$\int_0^L b\tau d_0\delta v'dx=\left[b\tau d_0\delta\left(v\right)\right]_0^L-\int_0^L bd_0\tau'\delta\left(v\right)dx=0\,, \tag{C7}$$

$$\int_0^L ab^2e\tau'\delta u_2'dx=\left[ab^2e\tau'\delta u_2\right]_0^L-\int_0^L ab^2e\tau''\delta u_2dx=0\,, \tag{C8}$$

$$\int_0^L ab^2e\tau'\delta u_1'dx=\left[ab^2e\tau'\delta u_1\right]_0^L-\int_0^L ab^2e\tau''\delta u_1dx=0\,, \tag{C9}$$

$$\int_0^L ab^2e\tau' d_0\delta v'' dx=\left[ab^2e\tau'd_0\delta v'-ab^2e\tau''d_0\delta\left(v\right)\right]_0^L+\int_0^L ab^2e\tau'''d_0\delta\left(v\right)dx=0\,. \tag{C10}$$